26th INTERNATIONAL CONGRESS ON SOUND AND VIBRATION
7-11 July 2019, Montreal

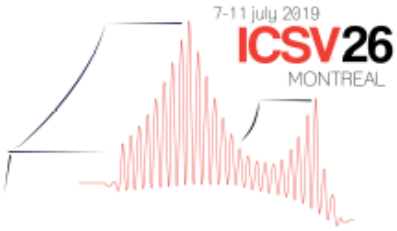

NUMERICAL INVESTIGATION OF THE FUNDAMENTAL LOW FREQUENCY MECHANISM OF THE OBJECTIVE OCCLUSION EFFECT: FOCUS ON THE EARCANAL WALL VIBRATION

Kévin Carillo, Olivier Doutres
École de technologie supérieure, Montréal, Québec, Canada
email: kevin.carillo.1@ens.etsmtl.ca

Franck Sgard
IRSST, Montréal, Québec, Canada

The occlusion of the human earcanal is commonly associated with the so-called occlusion effect. This phenomenon is particularly uncomfortable at low frequency when wearing an intra-aural occlusion device in shallow insertion. In low frequency, the occlusion effect is objectively quantified as the acoustic pressure increase in the occluded earcanal compared to the open one. Fundamentally, the occlusion effect is governed by the change of earcanal acoustic impedance seen by its wall due to its occlusion. However, several factors influence the occlusion effect such as the occlusion device (e.g., type, fit, position in the earcanal), the stimulation (e.g., position and nature) and the earcanal anatomy (e.g., geometry and material properties of earcanal surrounding tissues). Compared to the first two aforementioned aspects, the latter has not been investigated yet because of experimental difficulty. However, it is important since the earcanal anatomy influences the earcanal wall vibration, which is the origin of the acoustic pressure generated in the earcanal. In this work, the influence of the earcanal surrounding tissues geometry on its vibration distribution is numerically studied. For this purpose, a full factorial design of experiment is conducted using a 2D axi-symmetric finite element model of an open and occluded outer ear. The occlusion is simplified to an infinite impedance defined at the ear-canal entrance. The influence of the earcanal vibration distribution on the occlusion effect and its fundamental mechanism is then investigated. In conjunction, an eletro-acoustic model is proposed to explain in a simplified way the trend of the finite element model results.
Keywords: occlusion effect, fundamental mechanism, earcanal vibration, finite element method

1. Introduction

The occlusion effect (OE) of the human outer ear is a common phenomenon significantly noticeable at low frequencies (LF, <1 kHz) when wearing a shallow inserted intra-aural occlusion device [1]. The OE is generally described as the increased wearer's perception of his/her own physiological noise. It is thus considered as a notable source of discomfort (e.g., [2]). The propagation of physiological noise is achieved by bone conduction to the cochlea through different pathways (e.g., [3]). In the LF range, the contribution of the outer ear pathway on the hearing by bone conduction is negligible when the ear is open while it becomes predominant in the occluded case [3]. The OE is objectively quantified as the increase of acoustic pressure in the occluded earcanal (EC) compared to the open one (e.g., [4], [5]).

Fundamentally, the acoustic pressure increase is governed by the change of EC acoustic impedance seen by its wall due to the occlusion (e.g., [6], [7]). However, several factors influence the OE (e.g., [4], [6], [1], [3], [5], [8], [9]) such as the occlusion device (e.g., type, fit, insertion depth), the stimulation (e.g., nature, position) and the EC anatomy (e.g., geometry and properties of EC surrounding tissues). Concerning this latter aspect, the main contribution on the EC acoustic pressure comes from the cartilaginous part [10]. This has been explained by the higher compliance of the EC cartilaginous part compared to that of its bony part. Thus, the vibration would be higher in the former than in the latter EC part [10]. Since the distribution of the EC wall vibration is particularly difficult to experimentally assess, its influence on the OE has not been investigated yet. In addition, factors contributing to the EC wall vibration distribution have not been studied. Sophisticated models of the OE can be helpful to examine this aspect.

Several studies have proposed models for the OE (e.g., [4], [6], [5], [7], [8], [11], [12]). Lumped elements models based on electro-acoustic (EA) analogy (e.g., [4], [6], [5], [7]) are historically the first OE models. These models simplify the description of the spatially distributed EC behaviour into localized constants. Indeed, in EA models, the whole EC wall vibration is idealized as one acoustic flow source (e.g., [6], [7]) or two [5] concentrated at a chosen position in the EC. Parameters of this source (amplitude and position) are generally adjusted in several way based on acoustic pressure measurement in open and occluded EC in order to provide accurate OE results. Since the distributed EC wall vibration is not accounted for in EA models, its influence on the OE has never been thoroughly investigated according to authors' knowledge. In consequence, the relation between the source parameters and the EC wall vibration is not clear. To overcome the EA models limitations, finite element (FE) models (e.g., [8], [11], [12]) of the OE have been recently developed. FE models allow to accurately account for a complex geometry, boundary conditions and stimulation. They compare well to measurement data (e.g., [8], [11], [12]) and are useful (i) to optimize occlusion device properties especially to mitigate the OE and (ii) to investigate OE mechanisms (e.g., [13]), in particular the influence of the EC wall vibration distribution.

In this work, the role of the EC wall vibration distribution on the OE is numerically investigated using a 2D axi-symmetric FE model developed by Brummund et al. [11]. The occlusion is however simplified to an infinite impedance defined at the EC entrance: the complex influence of the occlusion device (e.g., [13]) is not accounted for in order to focus on the LF fundamental mechanism of the OE (i.e. the EC cavity impedance change). Compared to a 3D FE model, this 2D axi-symmetric model requires little computational resources. This facilitates the implementation of a 2^4 full factorial design of experiment (DOE) to investigate the variation of the EC wall vibration distribution and its influence on the OE. Parameters of this study focus on the geometry of the EC wall surrounding tissues. In conjunction, a simplified EA model is proposed in order to interpret in a simplified way the physics involved in the FE model. All inputs of the EA model, including the source parameters, are derived from the FE model.

2. Models of the occlusion effect

2.1 Finite element model

2.1.1 Axi-symmetric FE model of the outer ear

In this study, the 2D axi-symmetric FE model of the outer ear developed by Brummund et al. [11] is used as the reference model. In this model, shown in Fig. 1(a), the cylindrical EC, defined from its entrance to the tympanic membrane (TM), is surrounded by skin backed by cartilage and bone. Thicknesses of skin backed by cartilage and bone are respectively denoted as t_{cart} and t_{bone}. This model assumes that the proportion of EC skin which is backed by cartilage is equal to $\delta = 0.5$ while the remaining EC skin is backed by bone. The pinna is simplified to an extrusion of length l_{pinna} from the EC entrance made of skin (70%) and cartilage (30%) to preserve the axi-symmetry of the model. The EC entrance acoustic radiation in the surrounding environment is accounted for using the acoustic impedance of a baffled

circular piston. The TM is expressed using Shaw and Stinson's model [14] introduced as a locally reacting acoustic impedance. As previously mentioned, the occlusion is simplified to an infinite impedance defined at the EC entrance. Thus, the EC wall circumferential surface S_{EC} is equal in open and occluded cases. The system is excited by a unit normal and uniformly distributed force applied on horizontal boundaries of cartilage and bone tissues. Despite its simplifying assumptions, this model has been shown to compare well with experimental data [11]. All solid domains are assumed to exhibit linear elastic, isotropic material behaviour (properties detailed in Table 1). The air filling the EC is considered as non-dissipative fluid of properties ρ_0 and c_0 (see Table 1). All domains are meshed according to a convergence criterion of 6 elements per wavelength at 1 kHz using quadratic triangular elements. This model is solved using COMSOL Multiphysics 5.4 (© COMSOL Inc).

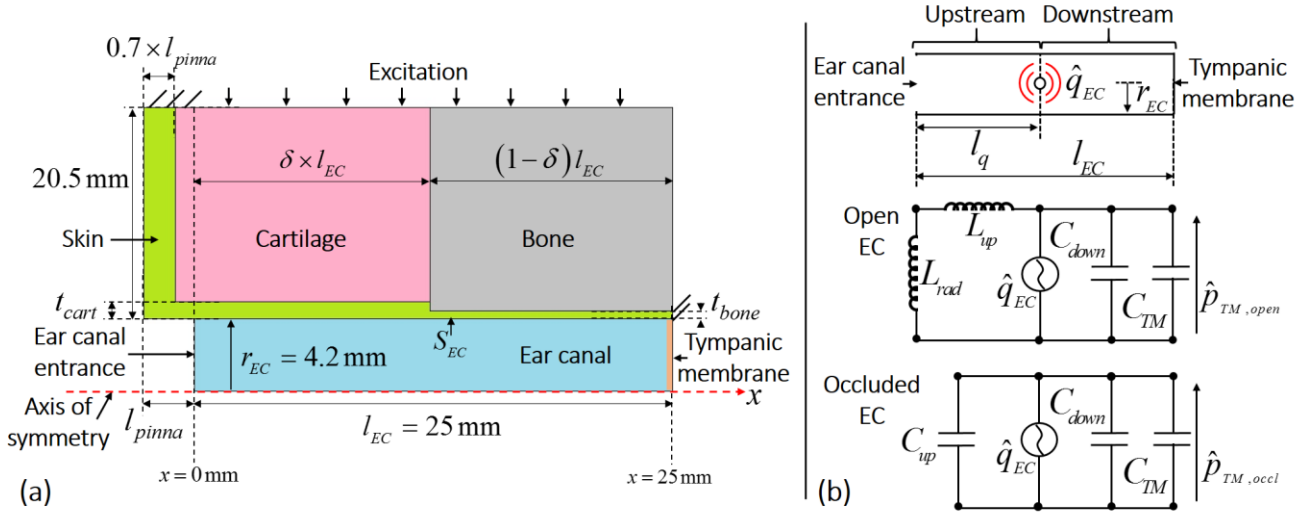

Figure 1: (a) 2D axi-symmetric FE model of the outer ear developed by Brummund et al. [11] and (b) EA model of open and occluded (using an entrance infinite impedance) EC.

Table 1: Properties of tissue domains used in the FE model. For the air filled EC cavity, density $\rho_0 = 1.2$ kg/m^3 and sound speed $c_0 = 343.2$ m/s were used.

	Density [kgm^{-3}]	Young's modulus [MPa]	Poisson's ratio [1]	Loss factor [1]
Bone	1714	11316	0.3	0.01
Cartilage	1080	7.2	0.26	0.05
Skin	1100	0.5	0.4	0.1

2.1.2 Computation of the vibro-acoustic indicators

The OE is computed as the difference between levels of the surface average TM acoustic pressure $< \hat{p}_{TM,k} >$ (where $k = \{open; occl\}$) in occluded and open ECs such as

$$OE = 20\log_{10}\left(\left|< \hat{p}_{TM,occl} >\right|\right) - 20\log_{10}\left(\left|< \hat{p}_{TM,open} >\right|\right). \quad (1)$$

The normal velocity distribution $\hat{v}_{n,EC,k}(x)$ along the EC wall is characterized by the position l_c of its centroid from the EC entrance computed such as

$$l_c = \frac{\int_0^{l_{EC}} x\left|\hat{v}_{n,EC,k}(x)\right| \mathrm{d}x}{\int_0^{l_{EC}} \left|\hat{v}_{n,EC,k}(x)\right| \mathrm{d}x}. \quad (2)$$

In addition, the EC acoustic impedance $\hat{Z}_{EC,k}$ defined as the ratio of the surface average EC wall acoustic pressure $<\hat{p}_{EC,k}>$ and the surface average EC wall normal velocity $<\hat{v}_{n,EC,k}>$ times the EC wall circumferential surface S_{EC} is calculated such as

$$\hat{Z}_{EC,k} = \frac{<\hat{p}_{EC,k}>}{<\hat{v}_{n,EC,k}> S_{EC}}. \tag{3}$$

2.2 Electro-acoustic model

Based on the previous FE model, an EA model inspired from Tonndorf's analogy [4] is proposed here and illustrated in Fig. 1(b). The EC is represented as a cylindrical duct of length l_{EC} and radius r_{EC}. The surface average EC wall normal vibration $<\hat{v}_{n,EC}>$, which is not influenced by the EC cavity load according to Brummund et al. [8], is associated with an ideal source of acoustic flow $\hat{q}_{EC} = <\hat{v}_{n,EC}> S_{EC}$. This source is concentrated at a distance l_q of the EC entrance. According to Fig. 1(b), the EC is schematically divided into two sections: (i) the upstream section defined from the EC entrance to the acoustic flow source and (ii) the downstream section defined from the acoustic flow source to the TM. When the EC is open, the volume of the upstream section is controlled in first approximation by its inertia effect represented by an acoustic mass L_{up}. The EC entrance radiation is accounted for using the acoustic impedance of a baffled circular piston reduced in first approximation to its inertia effect of acoustic mass L_{rad}. When the EC is occluded, the volume of the upstream section is rather governed in first approximation by its compressibility effect represented by an acoustic compliance C_{up}. In both open and occluded EC, the volume of the downstream section is controlled in first approximation by its compressibility effect of acoustic compliance C_{down}. Table 2 recalls the calculation of aforementioned acoustic masses and compliances. The TM is taken into account using the acoustic impedance of Shaw and Stinson's model [14] reduced in first approximation to its compressibility effect of acoustic compliance C_{TM} which is derived from its asymptotic LF behavior.

Table 2: Acoustic mass and compliance calculation for the EA model.

$L_{up} = \frac{\rho_0 l_q}{\pi r_{EC}^2}$	$L_{rad} = \frac{8\rho_0}{3\pi^2 r_{EC}}$	$C_{up} = \frac{l_q \pi r_{EC}^2}{\rho_0 c_0^2}$	$C_{down} = \frac{\left(l_{EC} - l_q\right)\pi r_{EC}^2}{\rho_0 c_0^2}$

Since the EA model (see Fig. 1(b)) considers that (i) both acoustic pressure at the TM and inside the EC are equal (LF assumptions inherent to the EA model) and (ii) position and intensity of the ideal acoustic flow source is not influenced by the EC cavity load, the OE can be written in terms of EC acoustic impedance seen by its wall (i.e. the acoustic flow source) in open and occluded cases by combining Eqs. (1) and (3) such that

$$OE = 20\log_{10}\left(\left|\hat{Z}_{EC,occl}\right|\right) - 20\log_{10}\left(\left|\hat{Z}_{EC,open}\right|\right). \tag{4}$$

In first approximation, $\hat{Z}_{EC,open}$ is governed by the acoustic mass of the EC upstream section given by

$$\hat{Z}_{EC,open} = j\omega\left(L_{up} + L_{rad}\right), \tag{5}$$

while $\hat{Z}_{EC,occl}$ is equal to

$$\hat{Z}_{EC,occl} = \left[j\omega \left(C_{up} + C_{down} + C_{TM} \right) \right]^{-1}. \quad (6)$$

Thus, according to Eqs. (4), (5) and (6), the OE can be explicitly expressed such as

$$OE = 20\log_{10}\left(\frac{1}{\omega^2}\right) - 20\log_{10}\left(L_{up} + L_{rad}\right) - 20\log_{10}\left(C_{up} + C_{down} + C_{TM}\right). \quad (7)$$

All EA model inputs (i.e. l_{EC}, r_{EC} and l_q) are derived from the FE model. In particular, the acoustic flow source is assumed here to be concentrated at the centroid position l_c ($l_q = l_c$) of the EC wall normal velocity computed at 100 Hz using the FE model. This assumption is evaluated in Section 3.

2.3 Configurations of interest

In order to investigate the distribution of the EC wall vibration and its influence on the OE, a 2^4 full factorial DOE is computed between 100 Hz and 1 kHz using the FE model in both open and occluded cases (32 simulations). The four parameters are δ (A), l_{pinna} (B), t_{cart} (C) and t_{bone} (D). The two levels (0 lower and 1 upper) of each parameter are detailed in Table 3. Levels of proportion δ (A) of EC backed by cartilage come from literature data which commonly reported 1/3 (e.g., [10]) to 1/2 (e.g., [11]). For the three remaining parameters (i.e. l_{pinna} (B), t_{cart} (C) and t_{bone} (D)), all levels are based on the literature review found in [11] related to the EC anatomy and adapted to the simplified EC geometry of the FE model. For each configuration, the centroid position of the EC wall normal velocity is computed using the FE model. This position is used as input data to the EA model to simulate the 32 configurations.

Table 3: Parameters (A, B, C, D) and levels (0, 1) of the 2^4 full factorial DOE.

	δ [1] (A)	l_{pinna} [mm] (B)	t_{cart} [mm] (C)	t_{bone} [mm] (D)
0	1/3	2	0.5	0.1
1	1/2	5	1	0.2

3. Results and discussions

In the following, the distribution of the EC wall vibration (Section 3.1) is only investigated using the FE model. Its influence on the EC cavity acoustic impedance (Section 3.2) and the OE (Section 3.3) is then studied using both FE and EA models. Results of the DOE in open and occluded cases computed using the FE model are presented in terms of standard deviation associated to mean value. In addition, the mean value obtained using the EA model is also displayed.

3.1 Velocity of the ear canal wall

The propagation through the outer ear of the vibration induced by the mechanical excitation force causes the vibration of the EC wall. The distribution of vibration along the EC can be represented by the position of its centroid l_c. Figure 2(a) shows that the centroid position of the open EC wall does not vary significantly (compared to the EC length $l_{EC} = 25$ mm) with frequency. Thus, the value of l_c at 100 Hz is considered in the remaining of this paper. Figure 2(b) displays the distribution along the open EC wall of its normal velocity at 100 Hz. To be comparable, the normal velocity is normalized by its surface average value since the vibration amplitude varies between all configurations of the DOE. According to Fig. 2(b), the vibration of the EC wall is maximum at the EC entrance and decreases with the position x along the EC. In particular, Fig. 2(b) shows that the EC wall vibration is concentrated into the cartilaginous part while the bony part does not vibrates significantly. This is qualitatively in agreement with the

literature (e.g., [10], [5]). In consequence, the centroid position l_c of the EC wall velocity is located in the cartilaginous part (mean value $\overline{l_c} = 3.9 \pm 0.7$ mm, see Fig. 2(b)). Analysis of the full factorial DOE results shows that the proportion δ of skin backed by cartilage has the main influence on the distribution of the EC wall vibration. Other parameters such as pinna length and skin thickness of cartilaginous and bony parts as well as interaction between parameters have a minor effect. From the EC entrance, the centroid position of the EC wall vibration increases with the proportion of skin backed by cartilage. Indeed, in average at 100 Hz, when the proportion δ increases from 1/3 to 1/2, the centroid position moves from 3.2 mm to 4.6 mm, which correspond to the limit values of the standard deviation (see Fig. 2(b)). Considering the EC length ($l_{EC} = 25$ mm), these variations are low. Substantially same results are obtained in the occluded case, not shown here for the sake of conciseness.

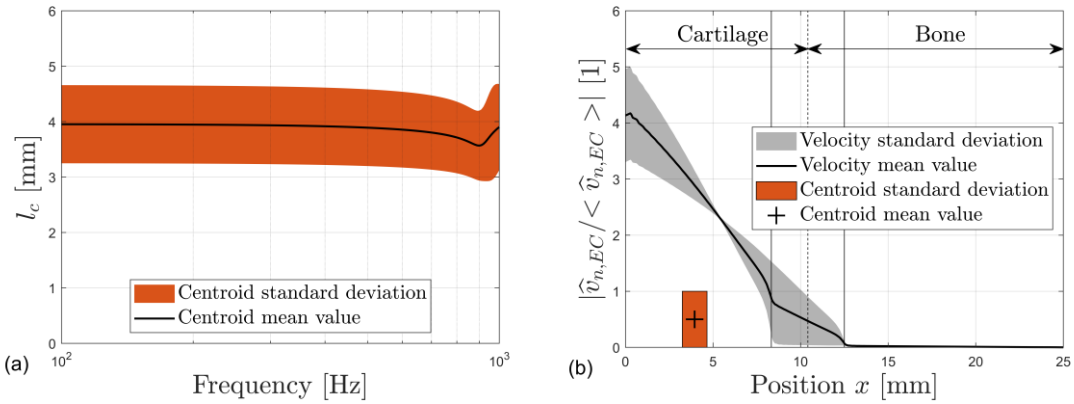

Figure 2: (a) Centroid position from the EC entrance of the open EC wall velocity as a function of frequency computed using the FE model and (b) distribution along the open EC wall of its normal velocity normalized by its surface average value computed using the FE model at 100Hz (vertical dotted line moves between the two vertical lines according to the proportion δ of skin backed by cartilage).

3.2 Acoustic impedance of the ear canal cavity

The vibration imposed to the EC cavity by its wall is responsible for the acoustic pressure generated in the EC. For a given EC wall vibration, the pressure generated depends on the EC cavity acoustic impedance seen by its wall (Eq. (3)). Figure 3(a) displays the surface average acoustic impedance level of the open and occluded EC cavity. Consider first the open case. Figure 3(a) shows that, for both FE and EA models, the open EC impedance level increases with frequency by + 20 dB/decade. From Eq. (5), the EA model indicates that the open EC acoustic impedance approximation is controlled by the acoustic mass of the EC upstream section comprised between the EC entrance and the acoustic flow source position. This acoustic mass represents the inertia effect of the open EC which depends on the source position (see Table 2). The latter has been assumed equal to the centroid position of the EC wall vibration ($l_q = l_c$). Because of the quasi perfect agreement between FE and EA predictions (see Fig. 3(a)), this assumption seems accurate. Figure 3(a) also shows that the open EC impedance depends on the distribution of the EC wall vibration (the standard deviation is not zero). However, since its centroid position does not significantly vary in the chosen range of parameters, the variation of the open EC impedance is not significant. Consider now the occluded case. Figure 3(a) shows that, for both FE and EA models, the occluded EC impedance level decreases with frequency by – 20 dB/decade. From Eq. (6), the EA model indicates that the occluded EC acoustic impedance is controlled by the acoustic compliance of the whole occluded EC. This acoustic compliance represents the compressibility effect of the occluded EC and does not depend on the position of the acoustic flow source. Indeed, from the FE model, the occluded EC impedance does not depend on the distribution of the EC wall vibration and its standard deviation, not

shown here, is zero. The slight difference in amplitude as the frequency increases between the occluded EC impedance level computed using FE and EA models (see Fig. 3(a)) is due to the approximation of the TM acoustic impedance to its compressibility effect in the EA model. In the open case, according to Fig. 3(a), the effect of the TM approximation is not observed between FE and EA models since the open EC impedance is controlled by the EC upstream section.

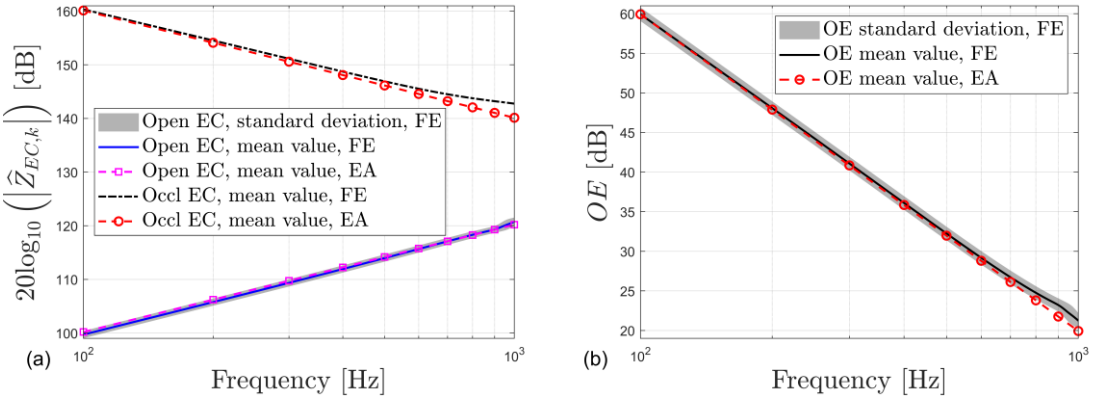

Figure 3: (a) Acoustic impedance level of the EC cavity seen by its wall as a function of frequency in open and occluded cases and (b) OE as a function of frequency.

3.3 Occlusion effect

The OE is computed according to Eq. (1) as the difference between the TM acoustic pressure level in occluded and open EC. In the EA model, the OE is given by Eq. (7). Figure 3(b) displays the OE as a function of frequency. Figure 3(b) shows that, for both models, the OE decreases with frequency by – 40 dB/decade which corresponds approximately, considering the assumptions made here and the experimental variability, to the typical trend of the OE (e.g., [5], [8]). This trend is the conjunction of the slope of the occluded EC acoustic impedance level (– 20 dB/decade) minus that of the open EC (+ 20 dB/decade). According to the EA model, the slope of – 40 dB/decade is completely described by the first term in Eq. (7) showing a dependence of the OE with the logarithm of the squared angular frequency inverse; this dependence being explained by the change of EC acoustic impedance between open and occluded cases (see Eqs. (4) and (5) respectively). The slight standard deviation associated to the open EC impedance level (see Fig. 3(a)) is consequently observed on the OE (see Fig. 3(b)). Indeed, the second term in Eq. (7) from the EA model exhibits the dependence of the OE to the open EC acoustic mass. The latter depends on the EC wall vibration distribution as demonstrated in the previous section. On the contrary, the distribution of the EC wall vibration does not influence the occluded EC impedance level (see Fig. 3(a)). The third term in Eq. (7) from the EA model indicates the dependency of the OE to the whole occluded EC compressibility. Thus, OE variability is entirely attributed to that of the open EC.

4. Conclusion

In this work, the LF fundamental mechanism of the OE has been revisited in the case of an acoustically rigid occlusion defined at the EC entrance using a 2D axi-symmetric FE model. In conjunction, an EA model has been proposed in order to explain in a simplified way the trend of the FE model results. In this simplified case, this study shows that the OE is directly governed by the change of EC cavity acoustic impedance seen by its wall between open and occluded cases. Using a 2^4 full factorial DOE focused on the geometry of the EC surrounding tissues, it is showed that the OE is slightly influenced by the variation of the EC wall vibration distribution. The latter is concentrated in the EC cartilaginous part. In the EA model, the distributed EC wall vibration is simplified to a concentrated acoustic flow source located at a particular position. Assuming that the latter corresponds to the centroid position of the EC wall normal

velocity, the EA model provides accurate results compared to those obtained with the FE model. In the occluded case considered here, it is showed that the occluded EC impedance does not depend on the EC wall vibration distribution since it is governed by the whole acoustic compressibility of the occluded EC. In the open case, the EC acoustic impedance is controlled by the acoustic mass defined from its entrance to the centroid position of the EC wall vibration. Results show that the latter mainly depends on the proportion of EC skin which is backed by cartilage. However, considering the limitations of the FE model used in this study, results presented here should be considered with caution. Indeed, the geometry of the EC and its surrounding tissues is simplified. In addition, the excitation, boundary conditions and material properties of the surrounding tissues are simplified. Thus, further investigation of the EC wall vibration distribution would require a more anatomically realistic FE model (e.g., [8], [15], [12]). Since the present study simplified the occlusion device to an infinite acoustic impedance defined at the EC entrance, future work should investigate the influence of the EC wall vibration distribution in conjunction to that of the occlusion device recently initiated by the authors [13].

REFERENCES

1 Berger E. H., Royster L. H., Driscoll D. P., Royster J. D., Layne M. (Eds.). (2003). *The Noise Manual (5th Ed)*. American Industrial Hygiene Association.

2 Kochkin, S. (2000). MarkeTrak V:"Why my hearing aids are in the drawer" The consumers' perspective. *The Hearing Journal*, ***53***(2), 34-36.

3 Stenfelt, S., & Goode, R. L. (2005). Bone-conducted sound: physiological and clinical aspects. *Otology & Neurotology*, ***26***(6), 1245-1261.

4 Tondorf, J. (1966). Bone conduction studies in experimental animals. *Acta Otolaryngologica*, ***132***(suppl 213), 7-9.

5 Stenfelt, S., & Reinfeldt, S. (2007). A model of the occlusion effect with bone-conducted stimulation. *International journal of audiology*, ***46***(10), 595-608.

6 Hansen, M. Ø., Poulsen, T., & Lundh, P. (1998). Occlusion effects, Part II: A study of the occlusion effect mechanism and the influence of the earmould properties.

7 Zurbrügg, T., Stirnemannn, A., Kuster, M., & Lissek, H. (2014). Investigations on the physical factors influencing the ear canal occlusion effect caused by hearing aids. *Acta Acustica united with Acustica*, ***100***(3), 527-536.

8 Brummund, M. K., Sgard, F., Petit, Y., & Laville, F. (2014). Three-dimensional finite element modeling of the human external ear: simulation study of the bone conduction occlusion effect. *The Journal of the Acoustical Society of America*, ***135***(3), 1433-1444.

9 Saint-Gaudens, H., Nélisse, H., Sgard, F., Laville, F., & Doutres, O. (2019). Comparison of different excitations to assess the objective occlusion effect measured on human subjects. *Proceeding of ICSV26*, Montreal, Qc, Canada, pp. 1-8.

10 Stenfelt, S., Wild, T., Hato, N., & Goode, R. L. (2003). Factors contributing to bone conduction: The outer ear. *The Journal of the Acoustical Society of America*, ***113***(2), 902-913.

11 Brummund, M. K., Sgard, F., Petit, Y., Laville, F., & Nélisse, H. (2015). An axisymmetric finite element model to study the earplug contribution to the bone conduction occlusion effect. *Acta Acustica united with Acustica*, ***101***(4), 775-788.

12 Poissenot, B., Benacchio, S., Sgard, F., & Doutres, O. (2019). An artificial ear to assess objective indicators related to the acoustical comfort dimension of earplugs: validation of a vibro acoustic model for insertion loss and occlusion effect assessment. *Proceeding of ICSV26*, Montreal, Qc, Canada, pp. 1-8.

13 Sgard, F., Carillo, K., & Doutres, O. (2019). A 2D Axisymmetric finite element model to assess the contribution of in-ear hearing protection devices to the objective occlusion effect. *Proceedings of Internoise*, Madrid, Spain, pp. 1-12.

14 Shaw, E., & Stinson, M. (1981). Network concepts and energy flow in the human middle‐ear. *The Journal of the Acoustical Society of America*, ***69***(S1), S43-S43.

15 Benacchio, S., Doutres, O., Le Troter, A., Varoquaux, A., Wagnac, E., Callot, V., & Sgard, F. (2018). Estimation of the ear canal displacement field due to in-ear device insertion using a registration method on a human-like artificial ear. *Hearing research*, ***365***, 16-27.